Fine Structure in the Absorption-Edge Spectrum of Si†*

G. G. MACFARLANE, T. P. MCLEAN, J. E. QUARRINGTON, AND V. ROBERTS
Royal Radar Establishment, Malvern, England

(Received May 2, 1958)

Measurements of the absorption spectrum of Si, made with high resolution, near the main absorption edge, at various temperatures between 4.2°K and 415°K, have revealed fine structure in the absorption on the long-wavelength side of this edge. This structure has been analyzed and can be interpreted in terms of indirect transitions involving, in general, phonons with energies corresponding to temperatures of 212°K, 670°K, 1050°K, and 1420°K. The form of the absorption associated with each type of phonon indicates that, as well as the formation of free electron-hole pairs taking place, excitons with a binding energy ~0.01 ev are produced in the absorption process. The temperature dependence of the indirect energy band gap has been found and using this along with data on the intrinsic carrier density indicates an increase with temperature of the combined density-of-states effective mass of the electrons and holes. A smoothing out of the basic features of the curves is observed and shown to be consistent with relaxation broadening. A discussion of the significance of the energies of the phonons taking part in the indirect transitions to the lattice vibrational spectrum of Si is given.

INTRODUCTION

IN a recent publication,[1] it was shown how the use of much higher optical resolution than had previously been available[2] revealed fine structure in the absorption spectrum of Ge near the main absorption edge. This fine structure was interpreted satisfactorily in terms of indirect optical transitions, and from it considerable information about the band structure and vibrational spectrum of Ge was obtained. As a continuation of previous work on the absorption spectrum of Si,[3] we have remeasured this spectrum under higher resolution and have resolved a fine structure near the main absorption edge similar to that in Ge. We have been able to explain this also in terms of indirect optical transitions. In this paper, we wish to discuss detailed analysis of this structure in the Si absorption curves and the information which can be obtained from it.

Although the methods of analysis used and the type of results found for Si are similar to those for Ge, we have been able to extend the analysis in Si to several features which we did not discuss in the case of Ge. We have succeeded in resolving the contributions to the indirect transitions not only from the two acoustical phonon branches but also from the two optical phonon branches in the ⟨100⟩ directions, these being the directions in which the Si conduction band minima are known to lie. It has been possible to find the detailed energy dependence of these contributions only for the two associated with the acoustical phonons; these two contributions contain knees which were discussed in I and shown to be characteristic of exciton producing indirect transitions. Furthermore, we have been able to study the smoothing out of these knees as the temperature increases and interpret it in terms of a temperature-dependent relaxation time of the excitons. Combining the intrinsic free-carrier concentration data and the temperature dependence of the energy gap obtained from our analysis, we have found, as for Ge, that the combined effective mass associated with the conduction and valence band edges increases with temperature. Also, the energies of the phonons taking part in the indirect transitions have been found; this leads to a further understanding of the lattice vibrational spectrum of Si and helps to fix the actual positions of the conduction band minima in k space.

In the following sections, we shall first of all discuss the details of the experimental procedure adopted in making the measurements followed by a presentation of the experimental results and a discussion of their analysis. Finally, we shall consider the information about excitons, band structure, and the lattice vibrational spectrum which can be deduced from this analysis.

EXPERIMENTAL PROCEDURE

The preparation of specimens and subsequent measurements were carried out in essentially the same way as described in I. Silicon specimens of approximate thickness 1.77, 0.381, and 0.0310 cm cut from very pure high-quality single crystals were polished and their transmission ratio I_T/I_0 was measured at a number of convenient fixed temperatures from 4.2°K to 415°K. Below room temperature, refrigerants having suitable known boiling points under normal atmospheric pressure were used to cool the specimen chamber. The specimen temperature was assumed for all practical purposes to equal that of the refrigerant, a preliminary experiment having shown that the thermal coupling through helium exchange gas is good enough to ensure this. At room temperature and above, the specimen temperature was measured directly by means of a calibrated copper-constantan thermocouple, the tem-

† A preliminary report on some of the results discussed in this paper was given at *The Fifth International Conference on Low-Temperature Physics and Chemistry, Madison, Wisconsin, August, 1957* (to be published), and a paper describing the work was read at the Spring (1958) Meeting of The Physical Society (London).

* This paper is published by permission of the controller, Her Britannic Majesty's Stationery Office.

[1] Macfarlane, McLean, Quarrington, and Roberts, Phys. Rev. **108**, 1377 (1957). We shall refer to the paper as I.

[2] G. G. Macfarlane and V. Roberts, Phys. Rev. **97**, 1714 (1955).

[3] G. G. Macfarlane and V. Roberts, Phys. Rev. **98**, 1865 (1955).

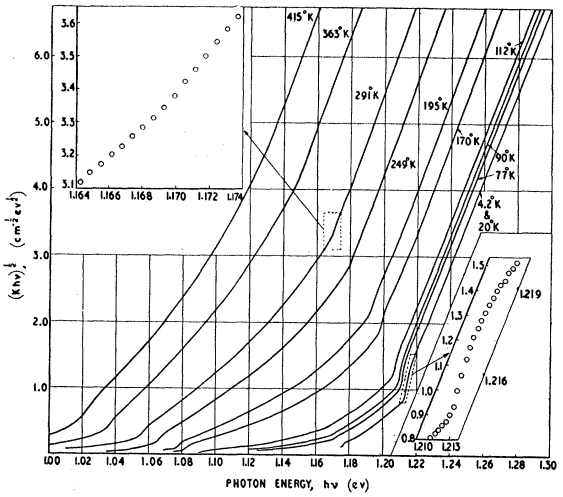

FIG. 1. Low-level absorption spectrum of high-purity Si at various temperatures. The inserts indicate the accuracy with which the experimental points define the curves.

perature being raised by electrically heating a high-boiling-point liquid in the absorption cell.

The radiation detector was a lead sulfide cell. The third-order spectrum from the diffraction grating was used, the spectrometer being calibrated using the several orders of the Hg green line (0.546074 micron.) In the absorbing region the slit widths ranged from 5×10^{-4} ev to 10^{-3} ev at the higher energies. Wavelengths λ were converted into energies E by the relation $E\lambda = 12400\times10^{-8}$ ev cm which may be compared with $E\lambda=(12397.8\pm0.5)\times10^{-8}$ ev cm given by Dumond and Cohen.[4]

Values of the absorption coefficient K were calculated from the relation

$$t=\frac{I_T}{I_0}=\frac{(1-R)^2\exp(-Kd)}{1-R^2\exp(-2Kd)},$$

where R is the surface reflectivity and d the specimen thickness. This reduces to $t_0=(1-R)/(1+R)$ when $K=0$, i.e., at energies below that of the absorption edge in a pure specimen at not too high a temperature, and this affords a means of deducing R as has already been mentioned in I. It should be noted that the value obtained for R, and indeed that measured for t at all levels of absorption, is subject to a slight uncertainty due to small changes in the optical path on moving the specimen into the radiation beam. One effect is that the distribution of light on the detector changes slightly, particularly with a thick specimen and when the absorption is low and multiple reflections become significant. It is clear therefore that, unless there is a very uniform distribution of sensitivity over the detector surface, a small uncertainty will be introduced into the measured transmission ratio. These difficulties were kept very much in mind since photoconductive cells are far from ideal in this respect and vary considerably from one to another. A cell specially selected for uniformity was used and the optical alignment was carried out in such a way as to minimize any errors of the kind mentioned.

As was found for Ge, the values of t_0 were greater than those deduced from the refractive index data of Briggs[5] by about 3% on the average, but were consistent among themselves to $\pm1\%$ for all specimens and at all temperatures. We are confident, therefore, that the uncertainties in t_0 are so small as to have a negligible effect on the subsequent analysis of the data. The reduction of the data for small values of t_0-t is discussed further in Sec. 2.

Routine reduction of the data and its tabulation in a suitable form for subsequent analysis was carried out by means of the laboratory's electronic computer.

RESULTS

The experimentally determined absorption curves are presented for a series of temperatures from 4.2°K to 415°K in Fig. 1 in the form of a plot of $\alpha^{\frac{1}{2}}\equiv(Kh\nu)^{\frac{1}{2}}$ against photon energy $h\nu$.[6] This set of curves has the same general characteristics as the similar set of curves for Ge described in I. At the lowest temperatures, the

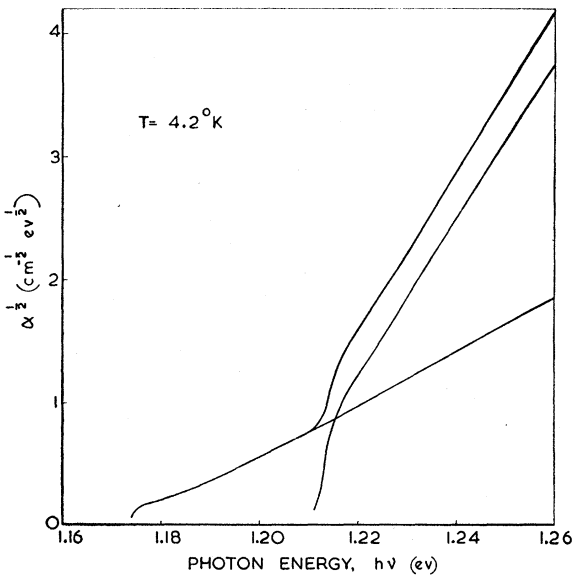

FIG. 2. The decomposition of the absorption coefficient at 4.2°K into its two components.

[4] J. W. M. Dumond and E. R. Cohen, Revs. Modern Phys. **25**, 691 (1953). *Note added in proof.*—All energy values in the present work and in I were derived from wavelength values appropriate to air and not vacuum. To correct for this, and for the discrepancy in the wavelength-energy conversion factor, all energy values should be divided by 1.00045.

[5] H. B. Briggs, Phys. Rev. **77**, 287 (1950).

[6] We shall work in terms of the more significant quantity α for Si rather than K as was done in I for Ge. It is more important to include the $h\nu$ factor in Si due to the larger energy range covered by the measurements.

TABLE I. The values of the threshold energies E_{1a}, E_{2a}, E_{3a}, E_{4a}, E_{1e}, and E_{2e} found from the analysis of the absorption curves, and the corresponding values of $\bar{E}$ at various temperatures, T. Also shown at each temperature are the values of θ_1 and θ_2 found from (2) and (3).

T (°K)	E_{4a} (ev)	E_{3a} (ev)	E_{2a} (ev)	E_{1a} (ev)	E_{1e} (ev)	E_{2e} (ev)	θ_1 (°K) $=T\log(\alpha_{1e}/\alpha_{1a})$	θ_1 (°K) $=(E_{1e}-E_{1a})/2k$	θ_2 (°K) $=T\log(\alpha_{2e}/\alpha_{2a})$	θ_2 (°K) $=(E_{2e}-E_{2a})/2k$	$\bar{E}$ (ev)
4.2					1.1740	1.2135					1.1558
20					1.1740	1.2135					1.1558
77					1.1715	1.2110					1.1532
90				1.1335	1.1705	1.2100	215	212			1.1522
112			1.0917	1.1312	1.1677	1.2072	198	212	657	670	1.1494
170			1.0827	1.1224	1.1588	1.1985	213	211	679	672	1.1407
195	1.0134	1.0453	1.0777	1.1172	1.1537	1.1932	225	212	686	670	1.1355
249	1.0015	1.0334	1.0660	1.1055	1.1420	1.1815		212		670	1.1237
291	0.9912	1.0231	1.0557	1.0952	1.1317	1.1712		212		670	1.1135
363	0.972	1.003	1.036			1.151				667	1.093
415	0.957	0.988	1.021			1.137				672	1.079

curves appear to consist of two components each beginning with a well-defined knee. As the temperature increases, two other components begin to appear at the low-energy end of the curves. These other components also have knees associated with them and it is seen from the figure that the energy separation of any pair of knees does not alter with temperature, e.g., the two outer knees have a constant separation of about 0.115 ev. As was discussed in I, these features are all characteristic of indirect optical transitions. For temperatures above 170°K, although the main features of the lower-temperature curves are still present, further absorption appears below the lowest-energy knee and increases with temperature. We shall discuss first of all the curves at temperatures up to and including 170°K where virtually no absorption occurs below the lowest-energy knee and follow this with a discussion of the curves at higher temperatures.

1. Temperatures Up to 170°K

The curves up to 170°K were analyzed using the same techniques of extrapolation, correlation, etc. as were described in I for Ge. It was found that they can in general be represented as the sum of four components, each component rising with energy from a different threshold energy and the two components with the lowest-energy thresholds disappearing at the lower temperatures. The decomposition of the curves at 4.2°K and 170°K into their components is shown in Figs. 2 and 3. At temperature T, we find that we can write $\alpha(h\nu,T)$ as

$$\alpha(h\nu,T)=\sum_{i=1}^{2}[\alpha_{ia}(h\nu-E_{ia}(T),T)+\alpha_{ie}(h\nu-E_{ie}(T),T)], \quad (1)$$

where

$$\alpha_{ie}(E,T)/\alpha_{ia}(E,T)=\exp(\theta_i/T) \quad (2)$$

and

$$E_{ie}(T)-E_{ia}(T)=2k\theta_i, \quad (3)$$

k being Boltzmann's constant. The absorption in this region can therefore be interpreted as being due to indirect transitions involving phonons of energies $k\theta_1$ and $k\theta_2$. Corresponding to the phonon of energy $k\theta_i$, there is a component of absorption α_{ia} beginning at $E_{ia}(T)$ in which a phonon is absorbed along with the light quantum, and a component α_{ie} beginning at $E_{ie}(T)$ in which a phonon is emitted. These two components have the same shape at a given temperature but differ in magnitude according to the relation (2). The components α_{1a} and α_{2a} disappear as the temperature is lowered and the number of phonons available for absorption decreases. The fixing of the threshold energies of the components is complicated by secondary effects which we shall discuss presently, but the values of θ_1 and θ_2 at the higher temperatures in the range can be readily obtained from the relation (2). The values of θ_1 and θ_2 so obtained are shown in the appropriate columns of Table I.

Indirect transition theory leads one to expect that

$$\alpha_{ia}(h\nu-E_{ia}(T),T)=a_i(T)[\exp(\theta_i/T)-1]^{-1}\alpha_i(h\nu-E_{ia}(T),T) \quad (4)$$

and

$$\alpha_{ie}(h\nu-E_{ie}(T),T)=a_i(T)[1-\exp(-\theta_i/T)]^{-1}\alpha_i(h\nu-E_{ie}(T),T), \quad (5)$$

where $a_i(T)$ is some weakly temperature-dependent factor which we define to be unity at zero temperature. We show here an explicit dependence of α_1 on T al-

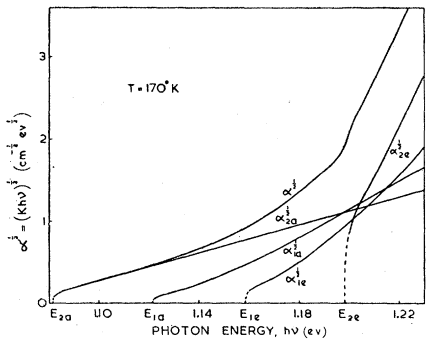

FIG. 3. The decomposition of the absorption coefficient at 170°K into four components.

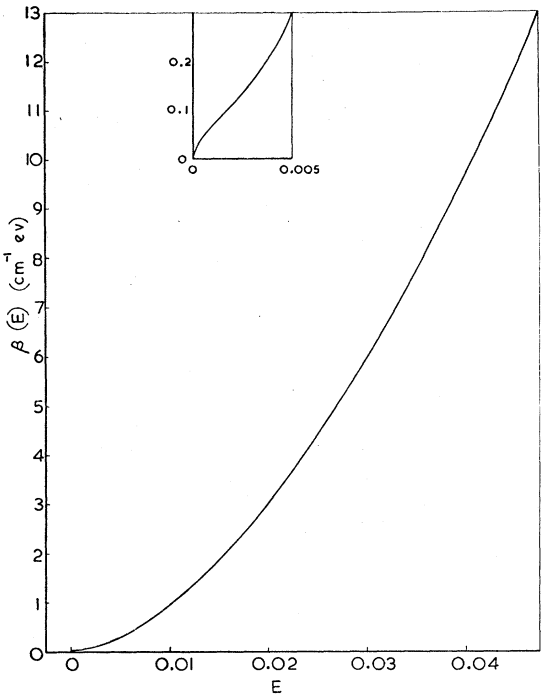

FIG. 4. The function $\beta(E)$. The insert shows the $E^{\frac{1}{2}}$ behavior of the function for small values of E.

though simple theory predicts only an implicit dependence on temperature through the temperature-dependent threshold energy. At 4.2°K, both the $a_i(T)$ and exponential terms in (5) are effectively unity, so that the two components comprising the absorption curve at this temperature represent α_1 and α_2 in both form and magnitude.

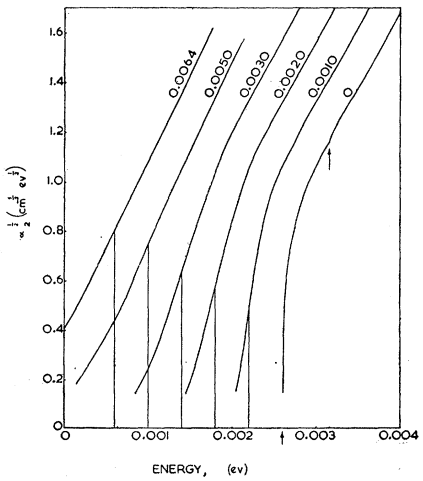

FIG. 5. The effect of Gaussian broadening on the basic shape α_2. Each curve is labeled with the appropriate half-width σ in ev and the vertical lines define the energy thresholds for the curves. The two arrows mark the threshold energies of the two components of the basic shape which rise as $(\Delta E)^{\frac{1}{2}}$ and which correspond to transitions to the ground and first excited states of the exciton.

As is seen from Fig. 2, both α_1 and α_2 begin with a well defined knee and eventually flatten off to rise roughly quadratically with energy. As the temperature is raised, however, these knees become smoothed out in a manner typical of relaxation broadening. This smoothing out can clearly be seen from the curves in Fig. 1. A detailed study of the variation of the shape of the knees in α_1 and α_2 with temperature showed that the variation can be explained by taking a basic shape which is subject to a temperature-dependent broadening of a Gaussian type. This broadening is applied of course to the whole component, but produces no significant change in shape in the upper region where the energy dependence is essentially quadratic. The basic shape of α_2, the larger component, is described empirically by

$$\alpha_2(h\nu-E_0)=18.08(h\nu-E_0)^{\frac{1}{2}}+\beta(h\nu-E_0-0.0055), \quad (6)$$

where absorption is measured in units of cm^{-1} and energy in ev. E_0 is the threshold for the component, and the function $\beta(E)$ which is shown in Fig. 4 behaves as $E^{\frac{1}{2}}$ for small values of E. At temperature T,

$$\alpha_2(E,T)=\frac{1}{\sigma(2\pi)^{\frac{1}{2}}}\int_0^\infty \alpha_2(x)\exp\left[-\frac{(x-E)^2}{2\sigma^2}\right]dx, \quad E>0, \quad (7)$$

where σ is a function of temperature and is a measure of the broadening of the basic shape. In Fig. 5 we show how the shape of α_2 changes with σ from $\sigma=0$, which is the curve defined by (6), to $\sigma=0.0064$ ev. The variation in the shape of the components α_{2a} and α_{2e} with temperature can be explained exceedingly well by using (4), (5), (6), and (7) with a suitable choice of σ at each temperature. The best value of σ at each temperature is shown in Table II. For the component α_1, the basic shape

$$\alpha_1(h\nu-E_0)=0.504(h\nu-E_0)^{\frac{1}{2}}+0.068\beta(h\nu-E_0-0.0055), \quad (8)$$

along with (4), (5), and (6) reproduces the experimental data well. It is clear that fitting the curves described by (4) to (8) to the various components at each temperature defines at these temperatures the energy thresholds E_{1a}, E_{2a}, E_{1e}, and E_{2e}. The values found in this way are given in Table I. It should be noticed at this point that these energy thresholds can be fixed accurately only if an analysis of the smoothing out of the basic shapes of the components, such as we have just discussed, is undertaken. This is especially true, as we shall presently see, in the high-temperature range where the smoothing out is much stronger and the components all have tails giving nonzero absorption at energies considerably smaller than the threshold energy. The values of the energy thresholds can be used in conjunction with Eq. (3) to yield values of θ_1 and θ_2, the phonon temperatures. The values of θ_1 and θ_2 found

TABLE II. The half-width σ of the Gaussian broadening and the corresponding relaxation time $\tau=h/\sigma$ at various temperatures, T.

T (°K)	4.2	20	77	90	112	170	195	249	291	363	415
$\sigma\times10^3$ (ev)	1.2	1.2	1.3	1.5	1.5	1.7	1.7	2.7	3.3	4.8	6.5
$\tau\times10^{12}$ (sec)	3.4	3.4	3.2	2.8	2.8	2.4	2.4	1.5	1.3	0.86	0.64

in this way are also shown in Table I; these values are more accurately determined than the corresponding values found by application of Eq. (2). The two pairs of components which comprise the absorption in this region appear to be associated with indirect transitions which involve the absorption and emission of phonons with energies equivalent to temperatures of about 212°K and 670°K. In Si, these phonons must have wave vectors lying in a ⟨100⟩ direction, this being the direction of the vector separating the valence and conduction band extrema in k space. From the ideas one can get about the vibrational spectrum of Si from the known elastic constants,[7] phonons with energies corresponding to these temperatures and with wave vectors lying in a ⟨100⟩ direction would appear to be acoustical.

2. Temperatures Above 170°

As we have already noted from Fig. 1, a considerable amount of absorption occurs for temperatures above 170°K at energies lower than the beginning, E_{2a}, of the lowest energy knee and the magnitude of this absorption increases with temperature. We show this part of the absorption on an expanded scale in Fig. 6. The curves are shown as continuous where the scatter in the experimental points is negligible but, at the lowest levels of absorption, the observed points are shown, as in this region the scatter on the points becomes unavoidably large. This scatter is due essentially to the fact that for these low absorption levels, the absorption coefficient is proportional to the difference of two large quantities. The actual values of these points depends very much on what one assumes the reflection losses in the crystal to be and it is worth while discussing how the points in Fig. 6 were obtained. We show in Fig. 7 a plot of the measured transmission ratio, t, as a function of the incident photon energy for two typical temperatures, 249°K and 363°K. The sudden drop in t at the high-energy end of these plots represents the beginning of absorption in the material. For energies lower than this, the transmission ratio falls slowly with increasing energy and can be well represented by a linear law. This fall represents a slow variation with photon energy of the reflection losses in the crystal. We have assumed that the linear variation in t due to these reflection losses continues into the higher energy region where absorption in the bulk of the material is also contributing to the variation in t, and so have extrapolated the straight line variation to higher energies. For low absorption levels, the absorption coefficient is just proportional to the difference (t_0-t) between the

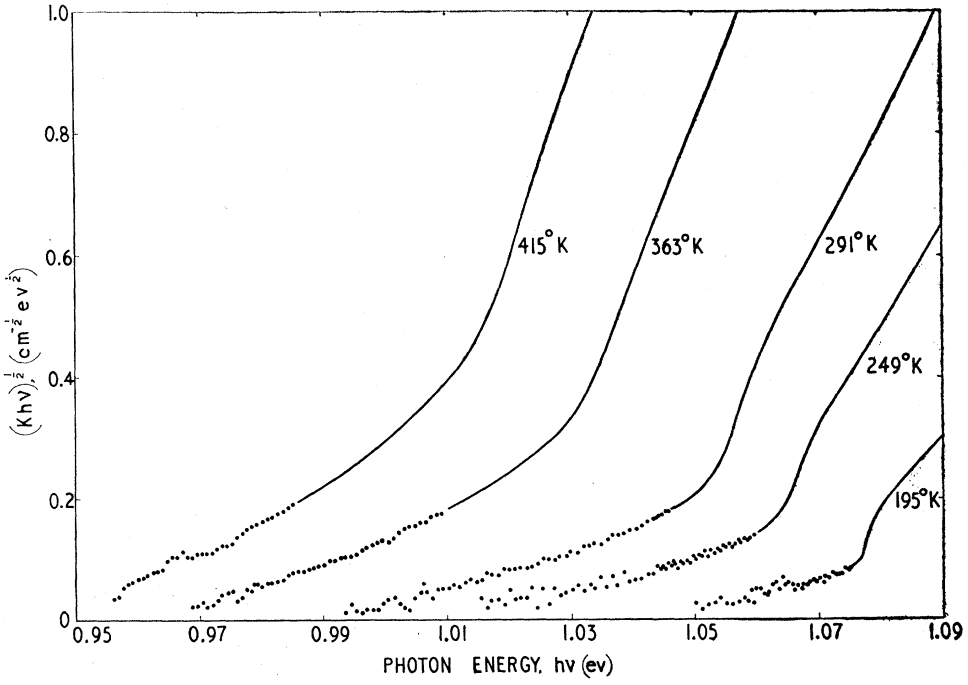

FIG. 6. Very low-level absorption spectrum of high-purity Si at various temperatures. At the upper levels, the experimental points define the curves unambiguously; at the lower levels, the experimental points are plotted.

[7] Y. C. Hsieh, J. Chem. Phys. 22, 306 (1954).

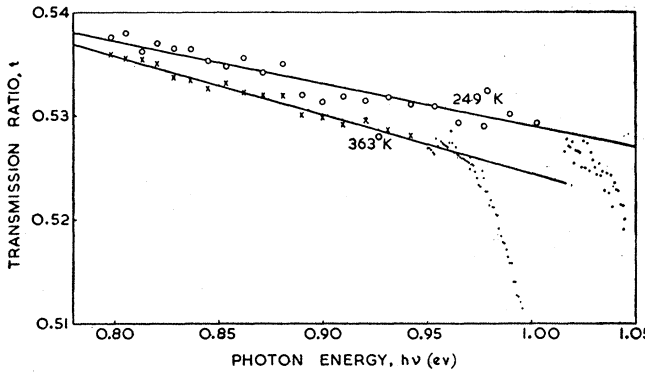

FIG. 7. The transmission ratio t as a function of photon energy at two typical temperatures over the energy range where bulk absorption begins.

transmission ratio t_0 due to reflection losses at a given energy and the measured value t of the ratio at that energy. The points on Fig. 6 were obtained by carrying out this differencing procedure from Fig. 7. Although the scatter in the measured values of t is seen from Fig. 7 to be at the most 0.5%, the differencing produces a much larger scatter in the corresponding values of K.

There is no very obvious structure in the absorption below the lowest energy knee, i.e., at energies less than E_{2a}, but it is just possible to detect on the curves a change in curvature at an energy about 0.032 ev below the main rise in the lowest energy knee and to notice that, below this energy at 195°K, the absorption is effectively zero. This suggests that the absorption in this region consists of two components, one which begins at about $(E_{2a}-0.032)$ ev and which does not appear below 195°K, and a second which begins at some lower energy and which does not appear until at least 249°K. Such components could be due to indirect transitions involving the absorption of phonons from the two optical branches of the vibrational spectrum in a ⟨100⟩ direction. We attempted to fit the curves on the basis of this idea but, in doing so, were unable to use the usual techniques of extrapolation, correlation, etc. due to the relatively large scatter on the experimental points in this region. However, we were able to synthesize curves which fit the experimental results at the five temperatures above 170°K to within their scatter and which are based on the values of only two parameters, θ_3 and θ_4, the two optical phonon temperatures. In terms of these two parameters, the curves are composed of two components α_{3a} and α_{4a} which are given by

$$\alpha_{ia}(h\nu-E_{ia}(T),\,T) = [\exp(\theta_i/T)-1]^{-1}\alpha_i(h\nu-E_{ia}(T)), \quad (9)$$

where

$$E_{ia}(T)=E_{2a}(T)-k(\theta_i-\theta_2), \quad i=3,4 \quad (10)$$

is the threshold of the ith component and the basic shapes $\alpha_3(E)$ and $\alpha_4(E)$ have both been taken proportional to E^2. This choice of a quadratic energy dependence for the components was governed both by the shapes of the experimental curves and the energy dependence to be expected from indirect band-to-band transitions. Furthermore, it was found that a fit could be obtained only if tails were associated with the α_{2a} component consistent with the tails already found at lower temperature due to the broadening and smoothing out of the knees. We show in Fig. 8 the decomposition of the appropriate part of the absorption curve at 363°K. This shows the two components associated with the optical phonons and the lower end of the component α_{2a} which is consistent with the formulas quoted in the previous section with a broadening characterized by $\sigma=0.0048$ ev. The best values of θ_3 and θ_4 were found to be 1050°K and 1420°K, respectively, both values being uncertain by about ±20°K. The values of E_{3a} and E_{4a} are shown in Table I.

Having found components which involve optical phonon absorption processes, one immediately looks for the corresponding components in which optical phonon emission plays a part. These components should begin at energies $E_{2e}(T)+k(\theta_i-\theta_2)$, $i=3,4$, and should be larger in magnitude than the phonon absorption components by $\exp(\theta_i/T)$. However, calculating their magnitude from this and the observed phonon absorption component, we find that, when added to all the other components present at the higher energies, their presence would be shown by a change in slope in the $\alpha^{\frac{1}{2}}$ curves of only about 1%–2%. This is rather an insignificant amount of structure to hope to observe in a region when the main part of the absorption is due to transitions involving acoustical phonons and when the extrapolated energy dependence of these acoustical phonon components is not known to better than 1% or 2% accuracy. We are therefore unable to decide whether or not the phonon emission branches are present.

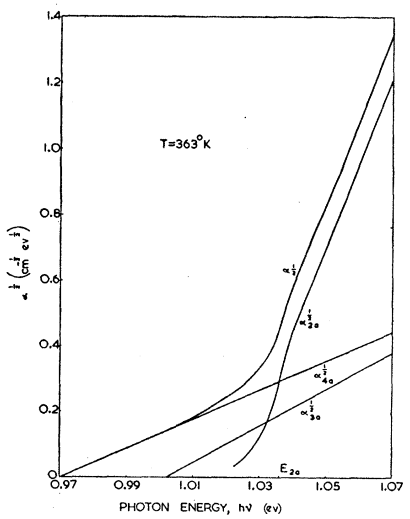

FIG. 8. The decomposition of the absorption coefficient at very low absorption levels at 363°K into the three components α_{4a}, α_{3a}, and α_{2a}. The shape of α_{2a} corresponds to the broadening of the basic shape (6) according to (7) with a half-width $\sigma=0.0048$ ev.

However, the evidence from the low-energy components seems sufficiently strong for us to conclude that they are in fact due to transitions accompanied by the absorption of optical phonons.

The main part of the absorption can be explained in terms of the two acoustical phonons which were found to take part in the transitions at the lower temperatures. This leads to values for the thresholds E_{1a}, E_{2a}, E_{1e}, and E_{2e}, and these are shown in Table I along with the values of θ_1 and θ_2 found at each temperature from both (2) and (3). At each temperature, the smoothing out of the structure is characterized by an energy σ which is given in Table II. There was no evidence for any significant variation of the factor $a_i(T)$ in (4) and (5) with temperature.

DISCUSSION AND CONCLUSIONS

1. General

The most obvious conclusion which can be drawn from the analysis just described is that, up to 415°K, the absorption is due to indirect optical transitions for low absorption levels (<50 cm^{-1}). Our knowledge of the band structure and symmetry properties of Si indicates that phonons of four different energies should contribute to these indirect transitions. These phonons should all have the same wave vector which should be in a ⟨100⟩ direction and, in order of increasing energy, should be transverse acoustical, longitudinal acoustical, longitudinal optical, and transverse optical. We have indeed found contributions to the absorption from phonons of four different energies, the best values of these energies corresponding to temperatures of 212°K, 670°K, 1050°K, and 1420°K. These energies are correct to about 1% in the case of the acoustical phonons and 2% in the case of the optical phonons. Haynes *et al.*[8] have analyzed the radiation emitted from the recombination of electron-hole pairs in Si and from this find values for the energies of the same four types of phonons as take part in the indirect transitions which produce absorption. They find the values 185°K, 640°K, 965°K, and 1380°K, which are in qualitative agreement with but consistently smaller than ours.

Associated with the transitions involving the emission and absorption of each type of phonon, there is an electronic energy gap for the process. If we denote by $E_i(T)$ the energy gap associated with the transitions involving the emission and absorption of phonons of energy $k\theta_i$, then

$$E_i(T)=E_{ie}(T)-k\theta_i=E_{ia}(T)+k\theta_1 =\tfrac{1}{2}[E_{ie}(T)+E_{ia}(T)] \quad (11)$$

for $i=1, 2, 3, 4$. Using the values of E_{ia}, E_{ie}, and θ_i given in Table I, one finds that $E_i(T)$ is independent of i as one might expect. Its value, denoted by $\bar{E}(T)$, is given in the last column of Table I and plotted as a function of temperature in Fig. 9.

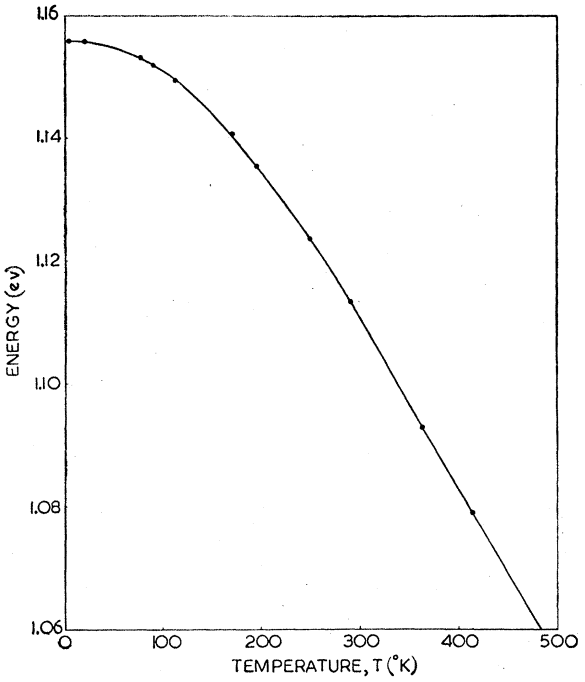

FIG. 9. The temperature dependence of $\bar{E}=E_G-E_{ex}$.

By using expressions of the type (4), (5), and (9), we can find the relative magnitudes of the basic shapes α_1, α_2, α_3, and α_4. The transitions giving rise to absorption are due to two different interactions, the interaction between the electrons and the incident radiation and that between the electrons and the vibrations of the crystal lattice. The interaction with the incident radiation is common to all the transitions giving rise to absorption in the components α_1, α_2, α_3, and α_4, and so these components differ in magnitude from one another due to the difference in the size of the coupling between the electrons and the various types of lattice vibrational modes in the crystal. If we characterize the coupling between the electrons and a lattice vibrational mode by C in such a way that the interaction Hamiltonian is proportional to this coupling constant, we find that

$$C_{\mathrm{LA}}\sim 5.5C_{\mathrm{TA}}\sim 4C_{\mathrm{TO}}\sim 4C_{\mathrm{LO}},$$

where C_{LA}, C_{TA}, C_{TO}, and C_{LO} are the coupling constants for the longitudinal acoustical, transverse acoustical, transverse optical, and longitudinal optical phonons, respectively; we have here assumed that the couplings to the two types of transverse acoustical and optical phonons are the same. We see therefore that, having extracted the phonon population factors from the interactions, the coupling of the electrons to the optical and the transverse acoustical modes are roughly all of the same strength, but about five times weaker than the coupling to the longitudinal acoustical modes.

[8] J. R. Haynes (private communication).

2. Band Structure and Excitons

The fact that the electronic energy gaps associated with the four types of phonons all turn out to be the same indicates that the electronic transitions producing absorptions at the threshold energy of each component are the same. To understand the nature of these transitions and the significance of the energy gap $\bar{E}(T)$, we must discuss the shapes of the various absorption components. We shall confine our discussion to the shapes of the two components α_1 and α_2 associated with the acoustical phonons, since the detailed shapes of the other two components α_3 and α_4 are not well known, especially close to their threshold energies. Disregarding the broadening effects, which are of secondary importance and which will be discussed later, the basic shapes of α_1 and α_2 are described by expressions (6) and (8). Both rise from their thresholds as $(\Delta E)^{\frac{1}{2}}$ and this energy dependence continues over the first 0.0055 ev. At this point another contribution begins and this also rises as $(\Delta E)^{\frac{1}{2}}$ initially but finally settles down to an almost quadratic energy dependence. This behavior is very similar to that found for the basic shape $g(E)$ in I for Ge and which was shown to be consistent with indirect exciton-producing transitions giving the initial rise as E^2, the eventual rise as E^2 being due to band-to-band transitions becoming the more important. A similar interpretation can be given to the two basic shapes α_1 and α_2, for, as Dresselhaus[9] and Elliott[10] have shown, the lowest exciton bands in Si have their minima at the same points in k space as does the conduction band; at these points, Dresselhaus estimates from the hole and electron effective masses the exciton binding energy to be $\sim$0.01 ev. The energy difference of 0.0055 ev, found from the analysis of α_1 and α_2, between the two contributions behaving as $(\Delta E)^{\frac{1}{2}}$ therefore represents the difference in energy of the ground and first excited states of the exciton. With a simple hydrogen model for the exciton, this interpretation leads to an exciton binding energy of 0.0073 ev, in agreement with Dresselhaus' estimate. It follows that the energy gap $E_G(T)$ for indirect band-to-band transitions at temperature T is given by

$$E_G(T)=\bar{E}(T)+E_{\text{ex}}, \tag{12}$$

where $E_{\text{ex}}\simeq$0.01 ev and is not expected to be temperature dependent. Figure 9 therefore shows the variation of E_G with temperature, but the values given by the curve are lower than E_G by about 0.01 ev. These values of E_G are consistently higher than those previously quoted.[3]

One other point should be mentioned about the shapes α_1 and α_2 and that is that one might expect them to contain contributions arising from transitions from the third valence band which is separated from the upper two by a spin-orbit coupling energy.[11,12] It has been estimated that at $k=0$ this band is lower than the other two by 0.03–0.04 ev, but to our knowledge no effects directly attributable to this third band have so far been observed. One would expect the presence of such a band to produce a component of absorption associated with every component arising from transitions from the upper two bands and having the same temperature dependence as these components, but beginning about 0.03–0.04 ev higher in energy than them. We had this fact very much in mind when we considered the extrapolation of the components on the original curves but could find no clear-cut evidence for such a second component being associated with α_1 and α_2.

We have also investigated, as in I, the relationship between the temperature dependence of the indirect energy gap, E_G, obtained from our measurements, and the intrinsic free-carrier density, n_i, obtained from electrical measurements. The theoretical relationship between these two quantities is

$$n_i=4.82\times10^{15}T^{\frac{3}{2}}(m/m_0)^{\frac{3}{2}}N_c^{\frac{1}{2}}\exp(-E_G/2kT), \tag{13}$$

N_c being the effective number of minima in the conduction band, m_0 the free electron mass, and $\bar{m}$ the combined density-of-states effective mass for holes and electrons. Experimentally, n_i has been found to vary as

$$n_i=AT^{\frac{3}{2}}\exp(-B/2kT). \tag{14}$$

Morin and Maita[13] found $A=3.87\times10^{16}$ and $B=1.21$ ev for temperatures above 450°K and Herlet[14] has found this relationship to hold down to 250°K. On the other hand, more recent work of Putley[15] has given the same temperature dependence for n_i but has reduced its magnitude by 20% for temperatures above 400°K. Taking E_G from (12) with $E_{\text{ex}}\sim$0.01, one finds from (13) that, with any of these values of n_i, the quantity $N_c(\bar{m}/m_0)^3$ must increase with temperature. It is fairly well established that the conduction band minima in Si lie inside the Brillouin zone and since they lie in the ⟨100⟩ directions, $N_c=6$. That they lie inside the zone agrees with the fact that we find four different phonon energies contributing to the indirect transitions. For minima at the zone edge, only three different phonon energies would be available, the longitudinal optical and acoustical branches being degenerate at the zone edge in the ⟨100⟩ direction. The value of $\bar{m}$ can be found at 4.2°K from the results of cyclotron resonance measurements at this temperature[12,16,17] and these give a value of $\bar{m}\sim0.45m_0$. With $N_c=6$, the n_i values of Morin and Maita indicate that $\bar{m}$ increases by about 45% over its value at 4.2°K as the temperature is in-

[9] G. Dresselhaus, J. Phys. Chem. Solids **1**, 15 (1956).
[10] R. J. Elliott, Phys. Rev. **108**, 1384 (1957).
[11] R. J. Elliott, Phys. Rev. **96**, 266 (1954).
[12] Dresselhaus, Kip, and Kittel, Phys. Rev. **98**, 368 (1955).
[13] F. J. Morin and J. P. Maita, Phys. Rev. **96**, 28 (1954).
[14] A. Herlet, Z. angew Phys. **9**, 155 (1957).
[15] E. H. Putley and W. H. Mitchell, Proc. Phys. Soc. (London) **A72**, 193 (1958).
[16] B. Lax and J. G. Mavroides, Phys. Rev. **100**, 1650 (1955).
[17] Dexter, Zeiger, and Lax, Phys. Rev. **104**, 637 (1956).

creased to 400°K. Putley's values indicate an increase by about 30% over the same temperature range. The magnitude of the increase is of course dependent on the value assumed for the exciton binding energy, but even assuming a zero binding energy the magnitude of the increase is reduced by only about 10% which still leaves a substantial increase in $\bar{m}$ with temperature. Although the indication of these calculations that $\bar{m}$ increases with temperature is probably true, the actual magnitude found for this increase seems rather large and is probably not reliable. This springs from the fact that in the calculation one takes the difference of the quantities B and E_G. This difference is much smaller than the quantities themselves and so one must know both B and E_G accurately. B, however, is known only to 0.01 ev whereas the difference amounts only to some thousandths of an electron volt.

A direct connection can be obtained between the variation with temperature of the energy gap and effective mass without resorting to the values of n_i. This can be done if a simple model is assumed for the temperature variation of the energy gap. This model assumes that the decrease in energy gap is simply due to a temperature-dependent scaling factor in the energy; states away from the band edge then approach the other band more quickly than those at the edge and the general effect is to flatten the bands and so increase their effective masses. On this model, the observed variation in energy gap with temperature leads to an increase in $\bar{m}$ of about 10% as the temperature rises from zero to 400°K.

3. Vibrational Spectrum

As we have already pointed out, the four phonons which assist in the indirect transitions must all have the same wave vector which, from the known band-structure of Si,[12] lies in a ⟨100⟩ direction; its actual position is somewhere inside the first zone and band-structure calculations[18] indicate that this position is in the outer half of the zone.

We have investigated how far the four energies found from our analysis can be explained in terms of the Born-von Kármán model of lattice vibrations developed for the diamond-type lattice by Smith.[19] It has recently been pointed out[20] that there is an error in Smith's work; the symmetry requirements of the diamond lattice are not as restrictive as implied by Smith and, instead of three, four parameters are required to describe a general force between an atom and its second-nearest neighbors. Smith set the fourth parameter equal to zero. However, it is easily shown that this fourth parameter does not enter into the expressions which describe lattice vibrations propagating along the symmetry directions. Consequently, Smith's expressions along these directions and for the elastic constants are correct.

It can easily be shown that, assuming noncentral harmonic interactions with nearest and second-nearest neighbors, two limits can be set on the acoustical vibrational energies at the zone edge in a ⟨100⟩ direction. These limits are determined by the lattice spacing, atomic mass, and elastic constants, and for Si are 320°K for the degenerate transverse branches and 477°K for the longitudinal branch. One can obtain force constants for this model which are sensible, viz., real, only if the two zone-edge energies of the acoustical branches are either both greater or both less than their respective limits. The longitudinal branch must certainly have an energy at the zone edge greater than the limit of 477°K, it already having a value of 670°K within the zone. However, it seems extremely unlikely that the transverse branches could increase from 212°K somewhere in the region of the zone edge to a value greater than the limit of 330°K at the edge. Thus it appears that the conditions cannot be satisfied which allow us to describe the Si lattice vibrational spectrum in terms of harmonic interactions with nearest and second-nearest neighbors only.

Using the slope at the origin of the longitudinal acoustical branch in a ⟨100⟩ direction obtained from the elastic constants and the fact that, at the zone edge in this direction, the longitudinal acoustical and optical branches of the spectrum meet one another with equal but opposite slopes, allows one to estimate the wave vector of the phonons of energies 670°K and 1050°K, assuming that it lies not too far from the zone edge.[18] We estimate that the wave vector lies at about 0.81 of the distance from the center to the edge of the zone, and this corresponds to the position of the conduction band minima in k space.

4. Broadening Effects

Our analysis shows that a considerable amount of broadening of the basic absorption shapes takes place and increases in magnitude as the temperature rises. This broadening was found to be of the Gaussian type characterized by a half-width σ which was found to vary with temperature as shown in Table II. Such a broadening is due to relaxation processes suffered by the particles in the crystal and, since the values of σ quoted in Table II refer to the broadening of that part of the absorption depending on the one-half power of the energy, these values of σ must characterize the relaxation processes undergone by the excitons. These same values of σ and even the Gaussian type of broadening need not apply and indeed would not be expected to apply to the upper parts of the absorption components, which are due to band-to-band transitions and whose broadening would be due to relaxation processes suffered by the electrons and holes.

[18] F. Herman, Physica **20**, 801 (1954); D. P. Jenkins, Proc. Phys. Soc. (London) **A69**, 548 (1956).
[19] H. M. J. Smith, Trans. Roy. Soc. (London) **A241**, 105 (1948).
[20] Braunstein, Moore, and Herman, Phys. Rev. **109**, 695 (1958).

To produce a broadening, these relaxation processes must be inelastic so that the exciton energy is changed when it undergoes such a process. We can characterize the frequency with which these processes take place by a relaxation time τ defined by

$$\tau = h/\sigma. \tag{15}$$

We give the values of τ at various temperatures in Table II and show its temperature dependence in Fig. 10. We see that τ is virtually constant around 3×10^{-12} sec for temperatures up to about 100°K, but above that it shows a marked decrease with increasing temperature. This is what one might expect since, for temperatures $T<100$°K, $kT<E_{ex}$ so that the exciton energy cannot be appreciably changed by interactions with the lattice vibrations and the relaxation must be due to some temperature-independent mechanism such as scattering by static imperfections in the crystal or the emission of phonons; as the temperature rises, the lattice vibrations become both more intense and more energetic and become the dominant scattering mechanism for the excitons and so lead to a relaxation time which decreases with increasing temperature. Finally, it should be pointed out that although the collision times τ_c for holes and electrons in good quality Si calculated from

$$\tau_c = (m^*/e)\mu, \tag{16}$$

where μ is the mobility and m^* an appropriate effective mass, have roughly the same order of magnitude as the relaxation times of the excitons, it does not seem appropriate to compare these times directly. This is due to the fact that first of all a certain amount of the temperature dependence of τ_c calculated from (16) comes from an averaging of the true collision time over the Maxwell-Boltzmann distribution of the holes or electrons; and secondly, the collision time characterizes processes, both elastic and inelastic, which alter the direction of motion of the particles but the relaxation time is concerned only with inelastic processes.

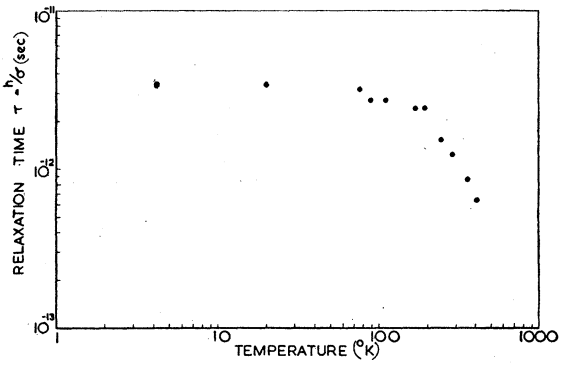

FIG. 10. The variation of the exciton relaxation time $\tau = h/\sigma$.

ACKNOWLEDGMENTS

We are most indebted to Mr. G. W. Green for growing the single crystals of Si. These were shaped and polished by Mr. J. D. Wilkinson who also assisted with the measurements. The digital computer was programmed by Mrs. D. G. Maisey. We also acknowledge the supply of liquid hydrogen and helium by Mr. C. A. Wright and his staff.